



**QUEEN'S
UNIVERSITY
BELFAST**

Modelling responses to spatially fractionated radiation fields using preclinical image-guided radiotherapy

Butterworth, K. T., Ghita, M., McMahon, S. J., McGarry, C. K., Griffin, R. J., Hounsell, A. R., & Prise, K. M. (2017). Modelling responses to spatially fractionated radiation fields using preclinical image-guided radiotherapy. *British Journal of Radiology*, (1069). <https://doi.org/10.1259/bjr.20160485>

Published in:
British Journal of Radiology

Document Version:
Publisher's PDF, also known as Version of record

Queen's University Belfast - Research Portal:
[Link to publication record in Queen's University Belfast Research Portal](#)

Publisher rights
Copyright the authors 2016.

General rights
Copyright for the publications made accessible via the Queen's University Belfast Research Portal is retained by the author(s) and / or other copyright owners and it is a condition of accessing these publications that users recognise and abide by the legal requirements associated with these rights.

Take down policy
The Research Portal is Queen's institutional repository that provides access to Queen's research output. Every effort has been made to ensure that content in the Research Portal does not infringe any person's rights, or applicable UK laws. If you discover content in the Research Portal that you believe breaches copyright or violates any law, please contact openaccess@qub.ac.uk.

Received:
1 June 2016

Revised:
15 July 2016

Accepted:
23 August 2016

<http://dx.doi.org/10.1259/bjr.20160485>

Cite this article as:

Butterworth KT, Ghita M, McMahon SJ, McGarry CK, Griffin RJ, Hounsell AR, et al. Modelling responses to spatially fractionated radiation fields using preclinical image-guided radiotherapy. *Br J Radiol* 2016; **89**: 20160485.

FULL PAPER

Modelling responses to spatially fractionated radiation fields using preclinical image-guided radiotherapy

¹KARL TERENCE BUTTERWORTH, PhD, ¹MIHAELA GHITA, PhD, ^{1,2}STEPHEN J MCMAHON, PhD,
^{1,3}CONOR K MCGARRY, PhD, ⁴ROBERT J GRIFFIN, PhD, ^{1,3}ALAN R HOUNSELL, PhD and ¹KEVIN M PRISE, PhD

¹Centre for Cancer Research and Cell Biology, Queen's University Belfast, Belfast, Northern Ireland, UK

²Department of Radiation Oncology, Massachusetts General Hospital and Harvard Medical School, Boston, MA, USA

³Radiotherapy Physics, Northern Ireland Cancer Centre, Belfast, Northern Ireland, UK

⁴Department of Radiation Oncology, University of Arkansas for Medical Sciences, Little Rock, AR, USA

Address correspondence to: Dr Karl Terence Butterworth

E-mail: k.butterworth@qub.ac.uk

Objective: Radiotherapy is planned to achieve the optimal physical dose distribution to the target tumour volume whilst minimizing dose to the surrounding normal tissue. Recent *in vitro* experimental evidence has demonstrated an important role for intercellular communication in radiobiological responses following non-uniform exposures. This study aimed to model the impact of these effects in the context of techniques involving highly modulated radiation fields or spatially fractionated treatments such as spatially fractionated radiotherapy (GRID).

Methods: Using the small-animal radiotherapy research platform as a key enabling technology to deliver precision imaged-guided radiotherapy, it is possible to achieve spatially modulated dose distributions that model typical clinical scenarios. In this work, we planned uniform and spatially fractionated dose distributions using multiple isocentres with beam sizes of 0.5–5 mm to obtain 50% volume coverage in a subcutaneous murine tumour model and applied a model of cellular response that

incorporates intercellular communication to assess the potential impact of signalling effects with different ranges.

Results: Models of GRID treatment plans which incorporate intercellular signalling showed increased cell killing within the low-dose region. This results in an increase in the equivalent uniform dose for GRID exposures compared with standard models, with some GRID exposures being predicted to be more effective than uniform delivery of the same physical dose.

Conclusion: This study demonstrates the potential impact of radiation-induced signalling on tumour cell response for spatially fractionated therapies and identifies key experiments to validate this model and quantify these effects *in vivo*.

Advances in knowledge: This study highlights the unique opportunities now possible using advanced preclinical techniques to develop a foundation for biophysical optimization in radiotherapy treatment planning.

INTRODUCTION

Radiotherapy treatment planning is based on the optimum delivery of physical dose to a target tumour volume. With the implementation of advanced conformal radiotherapy techniques such as intensity-modulated radiotherapy and stereotactic ablative radiotherapy into routine clinical practice, tumour volumes can be targeted with unparalleled accuracy and often using image guidance.

In addition to conformal radiotherapy techniques, spatially fractionated radiotherapy (GRID) delivers a single high dose fraction to the target volume in a non-uniform pattern, with subregions of the tumour exposed to high or low doses.¹ These are based on old approaches used to debulk large tumours with minimal toxicity, but nowadays can be delivered using advanced radiotherapy approaches through

either a custom GRID block,^{2–4} using a multileaf collimator⁵ and most recently using helical tomotherapy (TOMOGRID).⁶ GRID has been successfully used as part of palliative and curative treatments of large head and neck tumours, showing excellent initial response rates with low toxicity.^{2,7}

The complex, non-uniform dose distributions delivered during GRID therapy may be of significant importance to the underlying radiobiological mechanism of response. Using more simplistic approaches to generate non-uniform dose distributions *in vitro*, focused on the impact of steep dose gradients, our group has shown important contributions of non-targeted radiobiological effects driven by intercellular signalling, commonly known as bystander effects.^{8,9} Although classically associated with low dose

exposures, recent results have shown large contributions of signalling effects between cells exposed to high doses¹⁰ which remain in contact for extended periods,^{11–14} with reports of bystander cell killing of >50% and saturation doses >4 Gy.¹³ These observations have been supported by mathematical modelling studies which suggest that intercellular communication may have a significant role in cell death even in populations exposed to doses up to several Gy.^{15–18} Further evidence for these effects has been obtained in small animal models, showing effects of cell signalling *in vivo* for both tumour¹⁹ and normal tissue response.^{20,21}

However, whilst these experimental observations demonstrate the effects of intercellular communication *in vivo*, their role in tumour response following radiotherapy remains to be fully determined. The limited accuracy and precision associated with conventional preclinical radiation exposures has presented technical challenges in providing sufficiently accurate quantification that is needed for the validation of predictive models. With the implementation of precision image-guided radiotherapy devices in radiobiology research laboratories,^{22,23} it is now possible to systematically interrogate the physical parameters and underlying biological response mechanisms associated with heterogeneous radiation exposures and GRID.

This study aimed to simulate the impact of radiation-induced signalling effects on tumour cell killing and effective dose distributions for a range of different spatially fractionated treatment scenarios planned in small animal models. These predictions may have important treatment planning implications for GRID and can be used to identify experiments needed to determine the optimum parameters with which to validate tumour response models using small animal image-guided radiotherapy.

METHODS AND MATERIALS

Generation of treatment plans and dose calculations
Spatially fractionated treatment plans representative of typical GRID beam configurations were generated in Muriplan (Xstrahl Life Sciences, Camberley, Surrey, UK), a dedicated on-board treatment planning system small animals based on the superposition convolution algorithm.²⁴

Plans were generated based on the cone-beam CT reconstruction of a single representative subcutaneous tumour and aimed to achieve 50–60% coverage of the tumour volume (155 mm³) using circular beam sizes of 0.5- and 1-mm diameter and square fields of 3 × 3 and 5 × 5 mm². The number of isocentres and geometric configurations varied depending on the aperture size. The distance between the isocentres was in the range of 1 mm and different beam arrangements have been used as a function of the beam size. For 0.5- and 1-mm circular beams, a hexagon beam arrangement with 18 and 9 beams, respectively, was optimum to obtain 50% volume coverage. For 3 × 3- and 5 × 5-mm² beams, four and two isocentres were used to obtain similar tumour coverage. Plans were generated with equal prescribed doses at each isocentre using one beam per isocentre and then normalized to deliver equal mean doses to the whole tumour volume.

Cell response model

This work applies our published models describing cellular responses to modulated radiation fields incorporating cell cycling, cell arrest and DNA damage induced by both direct radiation exposure and indirect, cell signalling-mediated effects. Full descriptions of the model and its validation *in vitro* have been previously published^{16,17,25} and are briefly summarized below for completeness.

DNA damage in cells is quantified as discrete “hits”, representing potentially lethal damage. This damage can come about from two sources—direct radiation exposure and intercellular communication. In direct radiation exposures, hits are induced in cells with a Poisson distribution, with a mean number that is directly proportional to the delivered dose. Intercellular signalling can drive indirect signalling effects, where cells which respond to signal exposure see the induction of additional damage events which are treated identically to direct radiation-induced hits. The probability of a cell responding is taken to be a function of the time up to which it is exposed to these radiation-induced signals above some response threshold. This probability is independent of whether or not the cell was directly exposed to ionizing radiation, meaning signalling-driven damage occurs both in and out of field. In cells which respond to signalling effects, the amount of additional damage is taken to be Poisson distribution with a mean, which is a characteristic of the cell line.

It is assumed that cells secrete signals that can induce damage responses in neighbouring cells for a time proportional to the delivered dose. These signals are taken to be unstable, being removed from the system with exponential kinetics. For an isolated system (e.g. a tissue culture flask), this gives a signal concentration which initially builds to an equilibrium value before decaying away as cells cease signalling. By modelling the kinetics of this exposure, the total time for which cells are exposed to a given signalling level can be calculated and in turn used to determine the probability that a cell sees additional damage from signalling-driven effects.

These probabilities can be combined with the damage induced by direct radiation exposure to calculate cell survival, on either a cell-by-cell basis or population-level basis, and has been shown to agree well with experimental observations.^{16,17} Radiobiological response parameters for the DU-145 prostate cancer cell model were used based on radiation response characteristics determined in a previous work.¹⁷ These parameters were found to accurately reproduce the *in vitro* survival response described by the linear-quadratic parameters, $\alpha = 0.115$, $\beta = 0.026$.

Three-dimensional signalling

In a more complex system, such as a heterogeneously irradiated tissue, diffusion between subvolumes must also be taken into account. In previous work, we have assumed simple linear diffusion between neighbouring voxels,^{26,27} which is again applied in this work.

Specifically, for each plan under consideration, the CT scan and dose distribution obtained from the small-animal radiotherapy research platform system were extracted as Nearly Raw Raster Data (NRRD) files and imported into a custom MATLAB (Mathworks Inc, Natick, MA, USA) program, which extracted

the mouse target volume, as well as the dose delivered to each voxel. Voxels within the mouse were then simulated as uniformly exposed cell populations, with signals being allowed to diffuse between voxels within the mouse with a uniform diffusion coefficient. No signals were generated or diffused outside of the mouse volume. The diffusion coefficient within the mouse was set to simulate different signal ranges—this is the maximum distance from an irradiated volume at which a cell may see a signalling-induced damage response, as described previously.²⁷

For each irradiation condition and range, the level of survival has been calculated for each voxel within the tumour volume and compared with that predicted from a standard linear-quadratic dose response, assuming no interaction between neighbouring voxels. The dose which gives that level of survival in the linear-quadratic model is defined as the “signalling-adjusted dose”, for ease of comparison between different dose–volume histograms (DVHs). Specifically, signalling-adjusted doses are calculated as:

$$D_{\text{sig}} = \frac{-\alpha + \sqrt{\alpha^2 - 4\beta \ln(S)}}{2\beta}$$

where the signalling-adjusted dose for a given voxel, D_{sig} , depends on the model-predicted survival for that voxel, S , and the linear-quadratic parameters for uniform exposures α and β . This value can be both greater than the physical dose (e.g. in out-of-field cells which see signalling from higher dose regions) and lower than the physical dose (e.g. in small high-dose volumes whose signals are spread over larger volumes) depending on the physical beam geometry and signalling ranges.

These values were also converted into equivalent uniform doses (EUDs) for comparison between different exposures. For a given survival following a heterogeneous exposure, the EUD is the dose which would lead to the same level of survival if delivered uniformly to the whole volume. This is defined as

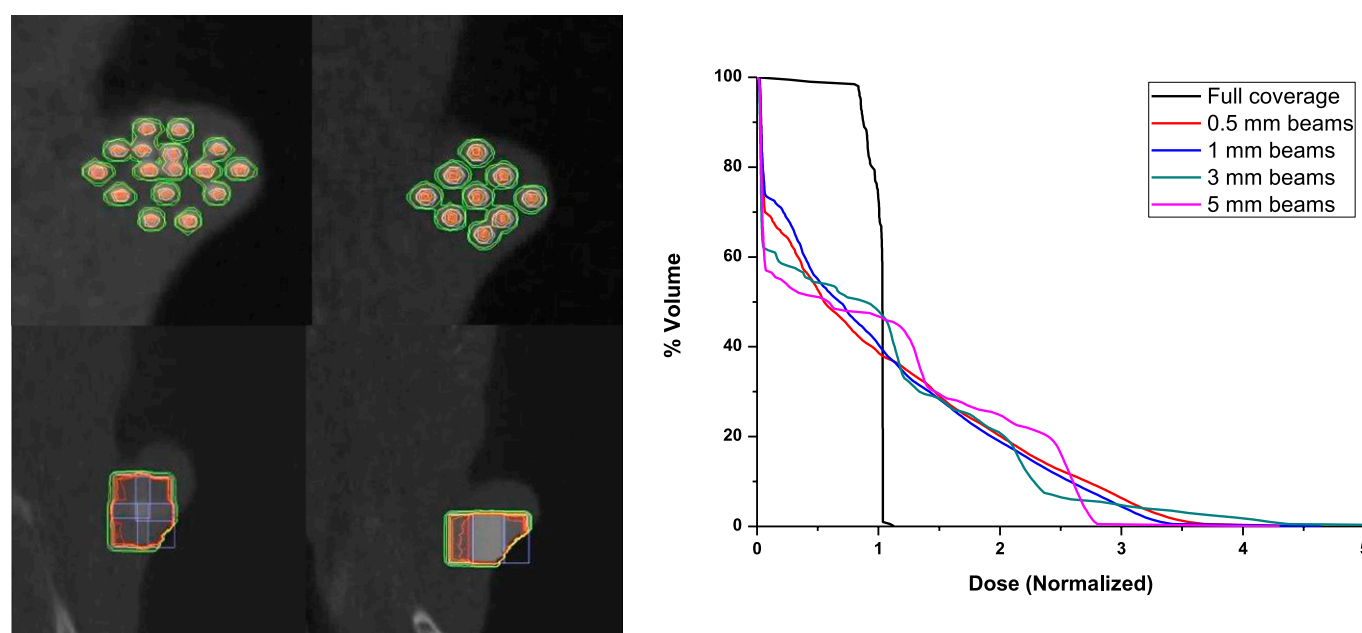
$$e^{-\alpha \text{EUD} - \beta \text{EUD}^2} = \frac{1}{N} \sum_{i=0}^N e^{-\alpha D_i - \beta D_i^2}$$

where the survival given by a dose of EUD is the same as the average cross all N voxels within the tumour volume, each exposed to a distinct dose D_i .

RESULTS

In this study, physical dose histograms (DVHs) for GRID treatments were designed to give an approximate tumour coverage of 50% under different spatial configurations using beam apertures from 0.5 to 5 mm. An example of the dose distributions generated in Muriplan is shown in Figure 1a for 0.5-mm isocentres along with the DVHs (Figure 1b) for each GRID plan generated using different beam sizes. For small beam sizes of 0.5 and 1 mm, approximately 30% of the outlined volume sees very low doses owing only to scattered radiation. In the remaining volume, there is a smooth increase in dose, caused by the large number of fields and high contribution of scatter owing to the small field sizes. This leads to highly heterogeneous dose distributions, with 60% of the volume seeing less than the mean dose and 10% of the volume seeing over three times the mean dose. In comparison, for larger square 3- and 5-mm beams, the DVHs show distinct structure, owing to the reduced number of

Figure 1. Treatment plans and dose–volume histograms (DVHs) for different spatially fractionated radiotherapy (GRID) beam arrangements generated with field sizes 0.5, 1, 3 or 5 mm: (a) Muriplan output for different GRID plans consisting of 16, 916, 9, 2 and 4 isocentres using a beam size of 0.5- and 1-mm diameter and 3×3 - and 5×5 -mm rectangular beams. The distance between isocentres ranges between 0.5 and 1 mm for the two beam geometries. Isodose lines show the 105% of prescribed dose in red and 15% of prescribed dose in green. (b) Physical DVHs for uniform full coverage plan and GRID plans generated with field sizes of 0.5, 1, 3 or 5 mm. All DVHs have been normalized to deliver the same average dose over the whole tumour.



fields and smaller scatter contribution in this scenario. Once again, a large portion of the volume ($\sim 40\%$) sees only negligible dose. Based only on physical dose, these cold spots should have a high probability of containing surviving cells in all irradiations.

Impact of intercellular signalling on dose-volume histogram for spatially fractionated radiotherapy treatment plans

Figure 2a–d present the intercellular signalling-adjusted DVHs for GRID plans with different beam sizes modelling various signalling ranges from 0.5 to 5 mm, with physical doses normalized to a mean dose of 5 Gy. As previously reported, at this dose,¹⁶ intercellular communication drives a considerable component of cell killing in low-dose regions. As a consequence, the largest difference between physical and signalling-adjusted doses across all beam sizes is in the low-dose regions, which only see negligible physical dose. Incorporating signalling-driven effects into the plan drives significant cell killing in these regions, which is in turn reflected in an increase in signalling-adjusted dose. Thus, in the

30–40% of the volume which receives a negligible physical dose, the inclusion of longer signalling ranges begins to fill in this dose valley, effectively increasing the cell killing and significantly reducing the potential survival of cells within this region. The dependence of this effect relies on the number and size of radiation fields used: whilst signalling in the small low-dose regions between the many 0.5-mm fields saturates almost immediately, it is not until ranges become comparable with the beam size that the 5-mm beams see a saturation of signalling effects.

For the highest dose regions, a small reduction in signalling-adjusted is seen, as damaging signals fall off more quickly in the heterogeneous scenario than the uniform exposure scenario typically assumed in the linear-quadratic analysis.

Mean dose and equivalent uniform dose for spatially fractionated radiotherapy treatment plans

Figure 3a shows the EUD for signalling in the 0–5-mm range calculated from the dose cloud and contoured volume data

Figure 2. Impact of cell signalling on dose-volume histograms (DVHs) for different spatially fractionated radiotherapy (GRID) plans generated using various beam sizes. Effective DVHs are produced for either 0-mm range (physical dose) or signalling ranges of 0.5, 1, 2, 3 and 5 mm for (a) 0.5-, (b) 1-, (c) 3- and (d) 5-mm beam size GRID. As signalling range increases, survival in the low-dose regions of the tumour falls significantly, which is reflected in an increase in the effective dose delivered to this volume in all plans. This effect is less rapid in large field plans, owing to the greater separation between beams.

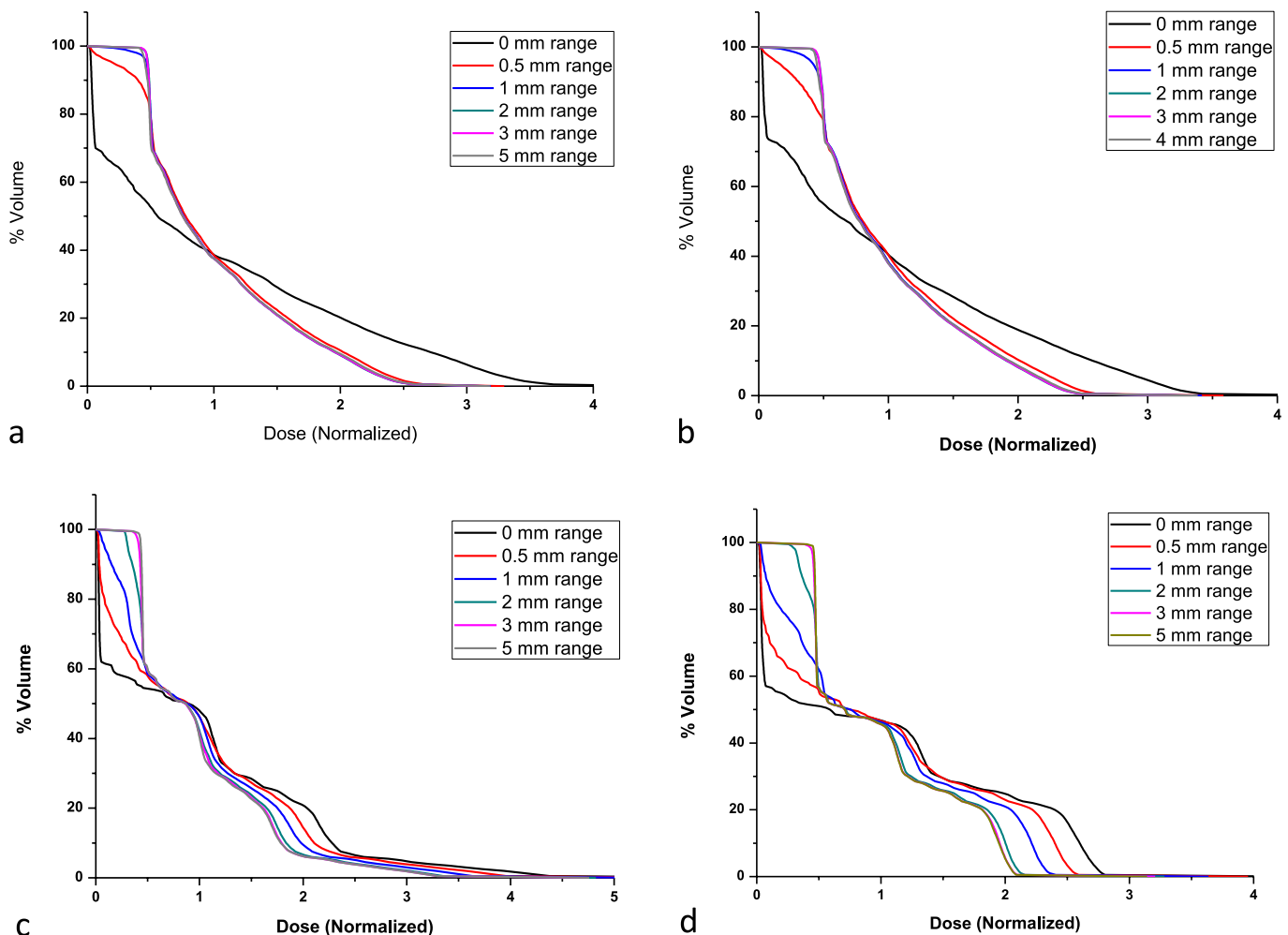
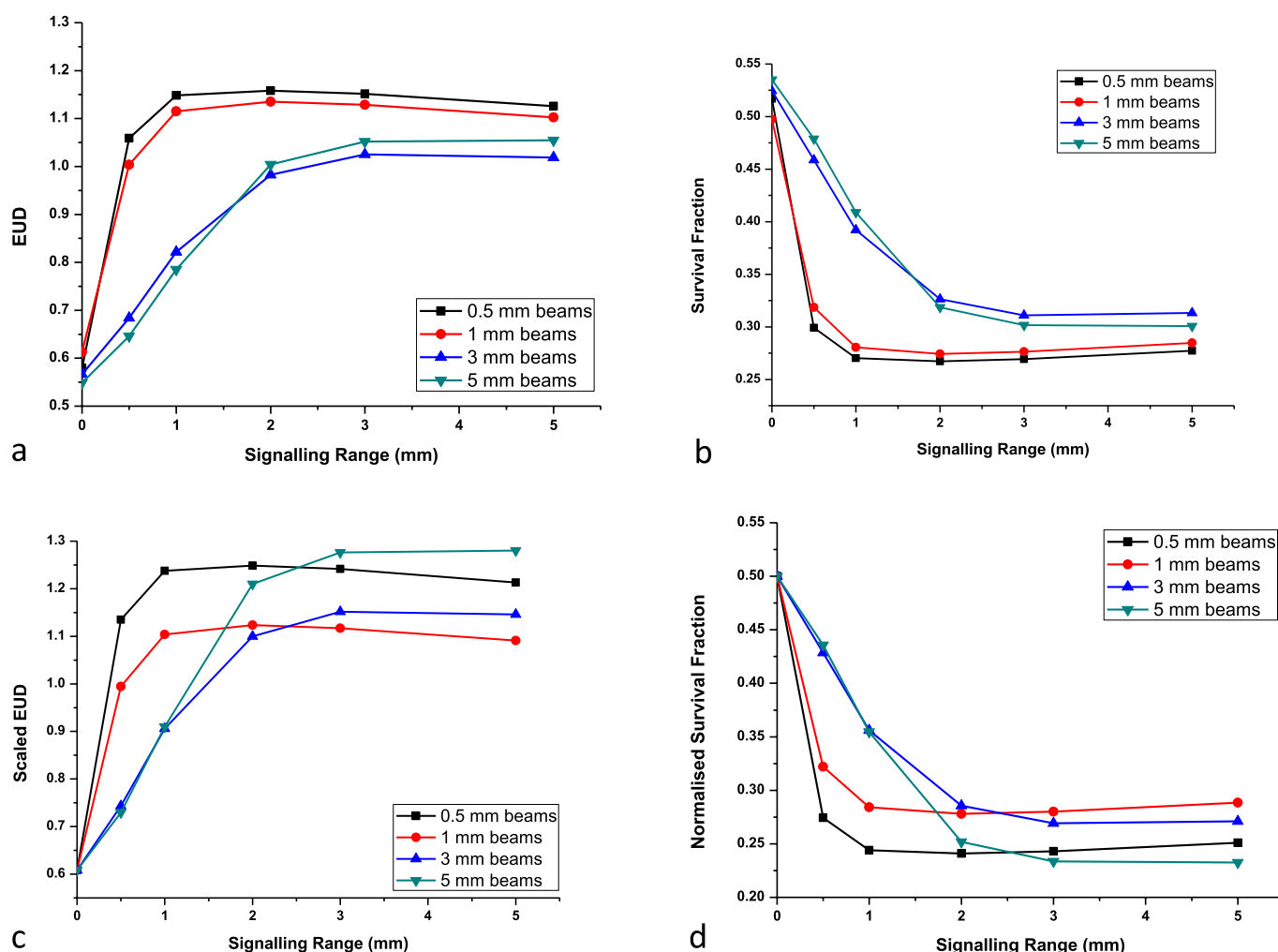


Figure 3. Impact of signalling range on calculated equivalent uniform doses (EUDs) and predicted surviving fraction. Changes in EUD and survival are presented for plans, normalized to deliver either equal physical dose (a, b) or identical EUD (c, d) in the 0-mm range case. For all conditions, incorporating signalling effects leads to a large increase in cell killing and corresponding increase in EUD, driven by reduced survival in the low-dose region of the tumour. This effect occurs much more rapidly for small fields than for exposures with fewer larger fields.



output from Muriplan, normalized to a 5-Gy mean dose, and Figure 3b shows the corresponding survival fraction. Owing to increased survival in the low-dose region of the target, the EUD in these plans is significantly lower than the mean dose. The EUD with no intercellular signalling varies with beam diameter: for 0.5-mm beams, the calculated EUD is 0.58 of the mean dose or 2.9 Gy, with a corresponding predicted survival fraction of 0.51, whilst 5-mm beams yield a survival of 0.55, corresponding to a normalized EUD of 0.55 (2.75 Gy).

However, when signalling is incorporated, cell killing in these low-dose regions increases significantly, reducing surviving fraction and increasing EUD. There is a clear separation between the small and large beam sizes, with a more rapid effect in the former. This is due to the different irradiated volume, where the many densely packed small fields see significant signalling in low-dose regions in the plans even at short signal ranges, whilst longer signal ranges are needed to fully expose the whole tumour to intercellular signalling for larger fields.

Small fields appear to cause systematically larger killing at all ranges in these analyses, but this is primarily a result of differences in EUD for equal mean doses in the no-signalling cases. To illustrate this, Figure 3c,d show the same results, but calculated by normalizing the EUD in the no-signalling case to an equal value, which in turn also gives identical survival in the absence of signalling, and similar behaviours for different field types at high signalling ranges.

Significantly, it can be seen that at high signalling ranges, the normalized EUD is >1 indicating that these highly heterogeneous dose distributions are causing greater cell killing than a uniform exposure delivering the same mean dose, even though a large fraction of the volume sees little or no dose. This is in stark contrast to traditional radiobiological models that assume cellular independence²⁸ and this may play an important role in the effectiveness of highly modulated therapies. This has important implications not only for the delivery of effective treatment regimens with modulated fields, but as yet undefined

consequences for our understanding of long-term radiation risk and mechanisms underpinning carcinogenesis where not only cell death will be important.

Lastly, at very long ranges, it can be seen that the EUD begins to trend down slightly, an effect which is driven by the gradual loss of signals from the irradiated volume to the surrounding normal tissue, somewhat reducing the cell kill expected for voxels exposed to the highest doses.

DISCUSSION

The goal of preclinical radiotherapy studies is ultimately to translate discovery through human trials and so, it is logical that the preclinical studies should be motivated and designed to align with a Phase 1 clinical trial. The capacity to model human radiotherapy trials in mice is not a trivial task but has much potential to provide further radiobiological understanding and improve the basis upon which trials in humans are designed.²²

The implication that the intercellular signalling effect plays an important role at clinically relevant doses has previously been investigated by McMahon *et al.*²⁶ Applying this Monte Carlo model of cellular radiation response to clinical plans resulted in a distortion in the dose distribution in organs near treatment fields, particularly in areas exposed to low doses.²⁶ This largely assessed the effects of intercellular signalling in the normal tissue outside the tumour and led to the conclusion that bystander signalling effects may play a more important role in relatively parallel organs sensitive to lower dose regions. A relatively smaller effect is typically seen in the high-dose regions that are typically the constraints in therapy planning.

The present study uses the same model of intercellular signalling effects but evaluates the effects within the tumour volume in the context of GRID treatment plans. In the traditional radiobiology paradigm that cells respond independently to ionizing radiation, the large dose valleys in GRID plans are expected to significantly reduce EUD. However, applying the theoretical model presented in previous work^{16,17} to different GRID treatment plans increases cell killing within the low-dose bath, which results in an increase in the EUD across the tumour. For some irradiation conditions, this can lead to an EUD which is significantly greater than that achieved by uniformly delivering dose to the tumour.

Furthermore, the cell kill within the tumour shows a different dependence on signalling range for different beam configurations, with smaller, more densely packed beams seeing much more rapid increases in cell killing than the more widely spaced larger beams. At high signalling ranges, the low-dose region in

both large and small beam plans sees significant levels of cell killing, and a small reduction in overall cell killing is seen in the high-dose regions, although this has only a limited effect on the total surviving fraction across the tumour as a whole.

Taken together, these effects indicate a potential approach to quantify the range these signalling effects have through *in vivo* preclinical radiobiological experiments, by comparing the effects on *in vivo* survival of tumour cells for equal physical doses delivered using uniform exposures or modulated fields delivered with small or large fields.

If signalling ranges are very short (<1 mm), then the uniform field will cause significantly greater cell killing than the modulated fields. If signalling ranges are intermediate (approximately 0.5–2.5 mm), small-field modulated delivery will cause cell killing similar to or greater than the uniform field, whilst the large fields will still see increased survival and reduced EUD. Finally, for large signalling ranges (>3.5 mm), all modulated fields will be expected to see significant increases in cell killing and EUD, comparable with or greater than uniform exposures.

Whilst the present theoretical study identifies a number of important potential impacts for radiation-induced signalling effects on tumour response to spatially fractionated radiotherapy, several other physical and biological factors may impact on tumour response. These include uncertainties in dose delivery associated with small field sizes and positioning accuracy. In addition, application of more advanced *in vivo* approaches using orthotopic or spontaneous tumour models that more accurately recapitulate aspects of the patient scenario would allow further insight into the underlying radiobiological mechanisms of response. Validating the scale of these effects *in vivo* will be an important step in the rational design of future clinical approaches which exploit these highly modulated exposures.

CONCLUSION

This study demonstrates the potential impact of radiation-induced signalling for complex spatially fractionated radiotherapy plans and also highlights how preclinical image-guided radiotherapy platforms have the potential to meaningfully probe the mechanisms of these effects, potentially providing invaluable data to support the development of future clinical trials.

FUNDING

SJM would like to thank the European Commission (EC FP7 grant MC-IOF-623630) for supporting his work. The authors are also grateful for support from the UK Department of Health (Ref 091/0205) and Friends of the Cancer Centre, Northern Ireland.

REFERENCES

1. Mohiuddin M, Fujita M, Regine WF, Megooni AS, Ibbott GS, Ahmed MM. High-dose spatially-fractionated radiation (GRID): a new paradigm in the management of advanced cancers. *Int J Radiat Oncol Biol Phys* 1999; **45**: 721–7. doi: [http://dx.doi.org/10.1016/S0360-3016\(99\)00170-4](http://dx.doi.org/10.1016/S0360-3016(99)00170-4)
2. Huhn JL, Regine WF, Valentino JP, Meigooni AS, Kudrimoti M, Mohiuddin M. Spatially fractionated GRID radiation treatment of advanced neck disease associated with head and neck cancer. *Technol Cancer Res Treat* 2006; **5**: 607–12. doi: <http://dx.doi.org/10.1177/153303460600500608>

3. Meigooni AS, Dou K, Meigooni NJ, Gnaster M, Awan S, Dini S, et al. Dosimetric characteristics of a newly designed grid block for megavoltage photon radiation and its therapeutic advantage using a linear quadratic model. *Med Phys* 2006; **33**: 3165–73. doi: <http://dx.doi.org/10.1118/1.2241998>
4. Buckley C, Stathakis S, Cashion K, Gutierrez A, Esquivel C, Shi C, et al. Evaluation of a commercially-available block for spatially fractionated radiation therapy. *J Appl Clin Med Phys* 2010; **26**: 3163.
5. Ha JK, Zhang G, Naqvi SA, Regine WF, Yu CX. Feasibility of delivering grid therapy using a multileaf collimator. *Med Phys* 2006; **33**: 76–82. doi: <http://dx.doi.org/10.1118/1.2140116>
6. Zhang X, Penagaricano J, Yan Y, Sharma S, Griffin RJ, Hardee M, et al. Application of spatially fractionated radiation (GRID) to helical tomotherapy using a novel TOMOGRID template. *Technol Cancer Res Treat* 2016; **15**: 91–100. doi: <http://dx.doi.org/10.7785/tcrteexpress.2013.600261>
7. Peñagaricano JA, Moros EG, Ratanatharthorn V, Yan Y, Corry P. Evaluation of spatially fractionated radiotherapy (GRID) and definitive chemoradiotherapy with curative intent for locally advanced squamous cell carcinoma of the head and neck: initial response rates and toxicity. *Int J Radiat Oncol Biol Phys* 2010; **76**: 1369–75. doi: <http://dx.doi.org/10.1016/j.ijrobp.2009.03.030>
8. Butterworth KT, McMahon SJ, Hounsell AR, O'Sullivan JM, Prise KM. Bystander signalling: exploring clinical relevance through new approaches and new models. *Clin Oncol (R Coll Radiol)* 2013; **25**: 586–92. doi: <http://dx.doi.org/10.1016/j.clon.2013.06.005>
9. Prise KM, O'Sullivan JM. Radiation-induced bystander signalling in cancer therapy. *Nat Rev Cancer* 2009; **9**: 351–60. doi: <http://dx.doi.org/10.1038/nrc2603>
10. Asur R, Butterworth KT, Penagaricano JA, Prise KM, Griffin RJ. High dose bystander effects in spatially fractionated radiation therapy. *Cancer Lett* 2015; **356**: 52–7. doi: <http://dx.doi.org/10.1016/j.canlet.2013.10.032>
11. Suchowerska N, Ebert MA, Zhang M, Jackson M. In vitro response of tumour cells to non-uniform irradiation. *Phys Med Biol* 2005; **50**: 3041–51. doi: <http://dx.doi.org/10.1088/0031-9155/50/13/005>
12. Mackonis EC, Suchowerska N, Zhang M, Ebert M, McKenzie DR, Jackson M. Cellular response to modulated radiation fields. *Phys Med Biol* 2007; **52**: 5469–82. doi: <http://dx.doi.org/10.1088/0031-9155/52/18/001>
13. Butterworth KT, McGarry CK, Trainor C, O'Sullivan JM, Hounsell AR, Prise KM. Out-of-field cell survival following exposure to intensity-modulated radiation fields. *Int J Radiat Oncol Biol Phys* 2011; **79**: 1516–22. doi: <http://dx.doi.org/10.1016/j.ijrobp.2010.11.034>
14. Butterworth KT, McGarry CK, O'Sullivan JM, Hounsell AR, Prise KM. A study of the biological effects of modulated 6 MV radiation fields. *Phys Med Biol* 2010; **55**: 1607–18. doi: <http://dx.doi.org/10.1088/0031-9155/55/6/005>
15. Ebert MA, Suchowerska N, Jackson MA, McKenzie DR. A mathematical framework for separating the direct and bystander components of cellular radiation response. *Acta Oncol* 2010; **49**: 1334–43. doi: <http://dx.doi.org/10.3109/0284186X.2010.487874>
16. McMahon SJ, Butterworth KT, McGarry CK, Trainor C, O'Sullivan JM, Hounsell AR, et al. A computational model of cellular response to modulated radiation fields. *Int J Radiat Oncol Biol Phys* 2012; **84**: 250–6. doi: <http://dx.doi.org/10.1016/j.ijrobp.2011.10.058>
17. McMahon SJ, Butterworth KT, Trainor C, McGarry CK, O'Sullivan JM, Schettino G, et al. A kinetic-based model of radiation-induced intercellular signalling. *PLoS One* 2013; **8**: e54526. doi: <http://dx.doi.org/10.1371/journal.pone.0054526>
18. Balderson MJ, Kirkby C. Potential implications on TCP for external beam prostate cancer treatment when considering the bystander effect in partial exposure scenarios. *Int J Radiat Biol* 2014; **90**: 133–41. doi: <http://dx.doi.org/10.3109/09553002.2014.868617>
19. Butterworth KT, Redmond KM, McMahon SJ, Cole AJ, Jain S, McCarthy HO, et al. Conventional in vivo irradiation procedures are insufficient to accurately determine tumor responses to non-uniform radiation fields. *Int J Radiat Biol* 2015; **91**: 257–61. doi: <http://dx.doi.org/10.3109/09553002.2014.980468>
20. Mancuso M, Pasquali E, Leonardi S, Tanori M, Rebessi S, Di Majo V, et al. Oncogenic bystander radiation effects in patched heterozygous mouse cerebellum. *Proc Natl Acad Sci U S A* 2008; **105**: 12445–50. doi: <http://dx.doi.org/10.1073/pnas.0804186105>
21. Mancuso M, Giardullo P, Leonardi S, Pasquali E, Casciati A, De Stefano I, et al. Dose and spatial effects in long-distance radiation signaling *in vivo*: implications for abscopal tumorigenesis. *Int J Radiat Oncol Biol Phys* 2013; **85**: 813–9. doi: <http://dx.doi.org/10.1016/j.ijrobp.2012.07.2372>
22. Butterworth KT, Prise KM, Verhaegen F. Small animal image-guided radiotherapy: status, considerations and potential for translational impact. *Br J Radiol* 2015; **88**: 20140634. doi: <http://dx.doi.org/10.1259/bjr.20140634>
23. Verhaegen F, Granton P, Tryggestad E. Small animal radiotherapy research platforms. *Phys Med Biol* 2011; **56**: R55–83. doi: <http://dx.doi.org/10.1088/0031-9155/56/12/R01>
24. Verhaegen F, van Hoof S, Granton PV, Trani D. A review of treatment planning for precision image-guided photon beam pre-clinical animal radiation studies. *Z Med Phys* 2014; **24**: 323–34. doi: <http://dx.doi.org/10.1016/j.zemedi.2014.02.004>
25. Partridge M. A radiation damage repair model for normal tissues. *Phys Med Biol* 2008; **53**: 3595–608. doi: <http://dx.doi.org/10.1088/0031-9155/53/13/014>
26. McMahon SJ, McGarry CK, Butterworth KT, O'Sullivan JM, Hounsell AR, Prise KM, et al. Implications of intercellular signaling for radiation therapy: a theoretical dose-planning study. *Int J Radiat Oncol Biol Phys* 2013; **87**: 1148–54. doi: <http://dx.doi.org/10.1016/j.ijrobp.2013.08.021>
27. McMahon SJ, McGarry CK, Butterworth KT, Jain S, O'Sullivan JM, Hounsell AR, et al. Cellular signalling effects in high precision radiotherapy. *Phys Med Biol* 2015; **60**: 4551–64. doi: <http://dx.doi.org/10.1088/0031-9155/60/11/4551>
28. Webb S, Evans PM, Swindell W, Deasy JO. A proof that uniform dose gives the greatest TCP for fixed integral dose in the planning target volume. *Phys Med Biol* 1994; **39**: 2091–8. doi: <http://dx.doi.org/10.1088/0031-9155/39/11/018>